

## A COMPACT, OPTOFLUIDIC SYSTEM FOR MEASURING RED BLOOD CELL CONCENTRATION

M. N. Gulari<sup>1</sup>, M. Ghannad-rezaie<sup>2</sup>, and N. Chronis<sup>1,2,3\*</sup>

<sup>1</sup>Macromolecular Science and Engineering, <sup>2</sup>Biomedical Engineering,

<sup>3</sup>Mechanical Engineering, University of Michigan, Ann Arbor, USA

### ABSTRACT

We developed a compact, single-cell imaging system for measuring red blood cell (RBC) concentration from diluted, whole blood samples. Key element of the design is the integration of a microfabricated lens array with a commercial haemocytometer. To image large areas and therefore a larger number of cells, the field of view (FOV) can be adjusted by simply increasing the thickness of the haemocytometer coverslip. We used a FOV = 200  $\mu\text{m}$ , corresponding to a resolution of 0.53  $\mu\text{m}$ , to demonstrate RBC counting: counts obtained from our system were in excellent agreement with counts obtained from standard microscopy and flow cytometry over a range of dilution factors.

### KEYWORDS

Red blood cell counting, optical imaging system, optofluidics, microfabricated lens array, haemocytometer.

### INTRODUCTION

Red blood cell (RBC) count, quantified as the number of cells per unit of blood volume, is an important clinical test that provides critical information about a patient's health status [1]. RBC in adults should be on the average of 4.2-6 million/ $\mu\text{L}$ . High RBC count (>6 million RBCs/ $\mu\text{L}$ ) can be the result of a chronic condition such as lung (pulmonary) disease, kidney cancer, or even smoking. Low RBC count is a typical sign of anemia which can be the result of internal bleeding, leukemia, bone marrow failure or even iron deficiency [1-2].

The most common methods for measuring concentration of RBCs in blood are based on flow cytometry and light microscopy. Flow cytometers, although extremely accurate, they are expensive, bulky instruments that require regular maintenance. On the other hand, light microscopy is an easy-to-use and cheap alternative that relies on the use a reusable device, called the haemocytometer that allows direct cell visualization. Haemocytometers cannot provide reliable counts as they suffer from human errors during the RBC counting process which is performed manually. Therefore a portable and accurate imaging system could make a significant contribution in monitoring pathological conditions that require RBC or other cell type counting, especially in resource-limited settings [3-5].

Several groups have been developing compact imagers for visualizing/counting biological samples over the last decade. Zhu et al. [6] demonstrated a cell phone-based fluorescence and dark field imager. The resolution of their system was in the range of 10-20 microns. Heng et al. [7] demonstrated a compact optofluidic microscope with high resolution that requires the sample to be scanned over a specially fabricated mask. Demirci et al.

[8-9] developed a lensless shadow imaging system for cell counting.

Here, we demonstrate a compact, high-resolution, optofluidic imaging system for visualizing and counting RBCs (Fig. 1). We call it 'optofluidic' because the core imaging unit is an array of microfabricated oil-immersion ball lenses. Its use is not limited to RBC counting: it can potentially be an ideal tool for imaging biological specimens in a resource limited setting or at the doctor's office, replacing bulky microscopes. Our portable system has a footprint of 7 cm x 7 cm and a total height of 6 cm.

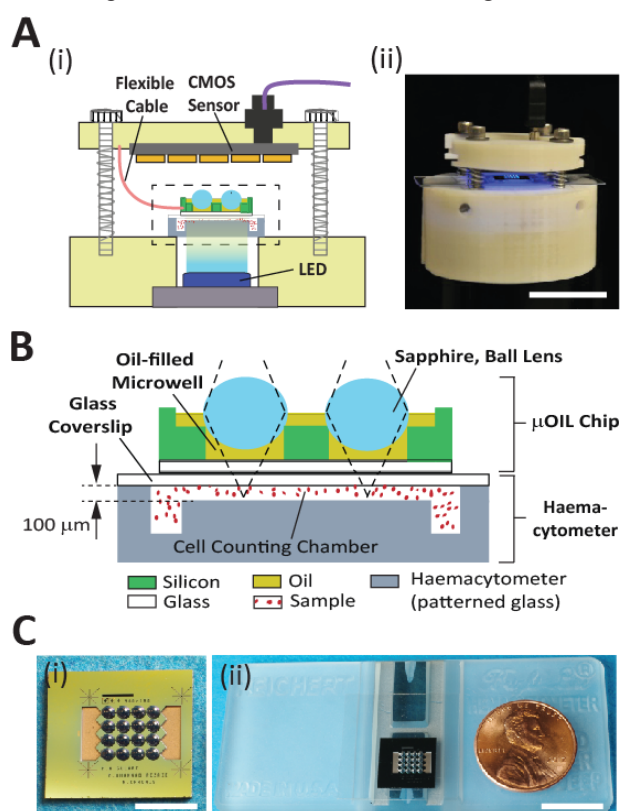


Figure 1. (A) The compact imaging system. (B) Schematic cross-section of the  $\mu\text{OIL}$  chip on top of a haemocytometer. Scale bar in (ii), 3 cm. (C) Pictures of the  $\mu\text{OIL}$  chip (i) and the  $\mu\text{OIL}$  chip/ haemocytometer assembly (ii). Scale bars, 5 mm in (i), 1 cm in (ii).

### METHODS

#### The $\mu\text{OIL}$ System

Our imaging system operates in bright field (transmission) mode and it consists of (Fig. 1A): (i) an array of Microfluidic-based Oil Immersion Lenses (termed 'the  $\mu\text{OIL}$  chip') [10], (ii) a commercially available haemocytometer, (iii) a low cost 5MP CMOS sensor (2.2 x 2.2  $\mu\text{m}$  pixel size) and, (iv) a blue LED. The haemocytometer is thick glass slide which forms a 100

$\mu\text{m}$  deep cell counting chamber (known as the Neubauer chamber) when a glass coverslip is placed on top of it. A custom-made plastic housing was manufactured to secure all those components in place except the haemocytometer that is manually inserted into the housing from the side.

The haemocytometer containing the blood sample is illuminated by the LED (centered at 470 nm) from below. The transmitted light is collected by the high numerical aperture (NA) lenses of the  $\mu\text{OIL}$  chip and is focused on the CMOS sensor that is placed 3-4 mm above the  $\mu\text{OIL}$  chip (Fig. 1B). To achieve a sharp, well-focused image, the exact distance between the  $\mu\text{OIL}$  chip and the CMOS sensor is manually adjusted using a set of screws. Finally, the CMOS sensor is connected to a computer that acquires and analyzes the image.

The  $\mu\text{OIL}$  chip (described in [10]) consists of 16 sapphire, ball lenses (1 mm in diameter, refractive index of 1.77) integrated on top of a 4x4 array of oil-filled microwells (Fig. 1C (i)). The oil/ball lens assembly forms a doublet lens and resembles the hemispherical front lens of an oil-immersion objective. The  $\mu\text{OIL}$  chip is placed directly on top of the haemocytometer (Fig. 1C (ii)). To achieve a good contact between the  $\mu\text{OIL}$  chip and the haemocytometer coverslip (and therefore eliminate any gap between them), a flexible cable is used as a spring to push the  $\mu\text{OIL}$  chip against the coverslip. As a result, the distance between the  $\mu\text{OIL}$  chip and the sample in the Neubauer chamber is always fixed.

The microfabrication of the  $\mu\text{OIL}$  chip is based on a two-step DRIE process for creating the microfluidic channels and the microwell array. A 100  $\mu\text{m}$  thick glass wafer is anodically bonded to the DRIE etched silicon. This extra microfabrication step has been added to the original microfabrication process [10] to eliminate chip to chip variations in the total thickness of the  $\mu\text{OIL}$  chip.

### Counting RBCs

We performed RBC counts with fresh whole, diluted blood samples on a commercial haemocytometer (Hausser Scientific) covered with a 150  $\mu\text{m}$  thick glass coverslip (Fig. 2A). The Neubauer chamber of the haemocytometer has a total volume of 6-7  $\mu\text{l}$  and it has a square grid pattern to facilitate the cell counting (Fig. 2B).

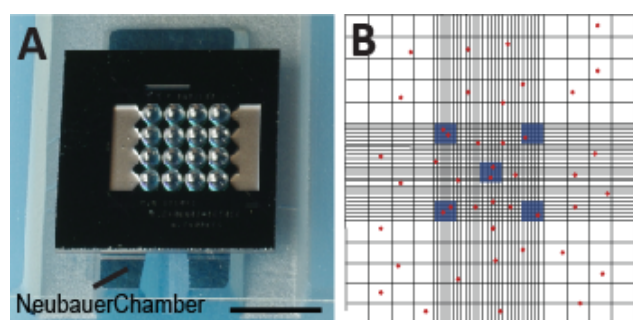


Figure 2. (A) The  $\mu\text{OIL}$  chip on top of the Neubauer chamber. Scale bar, 4 mm. (B) Schematic of the grid pattern that sits beneath the  $\mu\text{OIL}$  chip. The dark-colored boxes are 200  $\mu\text{m}$  x 200  $\mu\text{m}$  and represent the 5 regions where cells (red dots) are counted.

To image the haemocytometer and count the RBCs, we used: (i) a microscope (Olympus-BX51WI) in epi-illumination mode with a 50x objective (NA=0.5), connected to a 5 MP digital camera and, (ii) our compact imaging system with a field of view (FOV) of 200  $\mu\text{m}$  and a NA of 0.54. In this case, the distance between the cells and bottom surface of the  $\mu\text{OIL}$  chip was  $\sim 250$   $\mu\text{m}$  (RBCs tend to settle at the bottom of the Neubauer chamber). In all our imaging experiments, we used a single lens from the  $\mu\text{OIL}$  chip for consistency in the image quality.

Blood samples ( $\sim 10$   $\mu\text{L}$  in volume, diluted by a factor of 50, 100 and 200) were pipetted into the haemocytometer and driven in the Neubauer chamber by capillary action. Images of the blood samples were captured from 5 different 200  $\mu\text{m}$  x 200  $\mu\text{m}$  square areas in the grid pattern of the Neubauer chamber (marked as dark boxes in Fig. 2B). The dilution and imaging procedures used in our experiments are the recommended ones for haemocytometer-based RBC counting [11-12].

## RESULTS AND DISCUSSION

### FOV, Resolution of the $\mu\text{OIL}$ System

For cell counting applications, the FOV of each lens in our system is an important feature as it determines how much blood volume (and therefore how many cells) can be imaged.

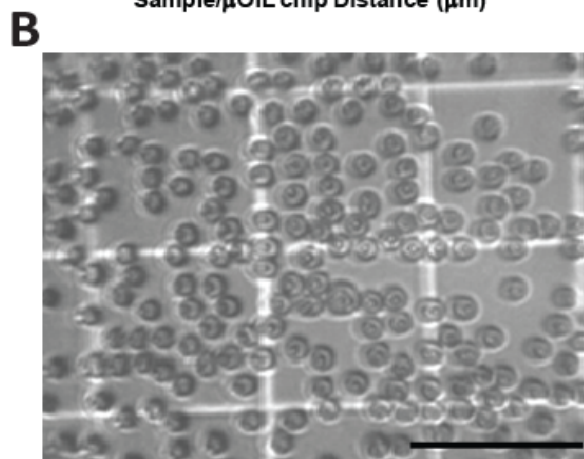
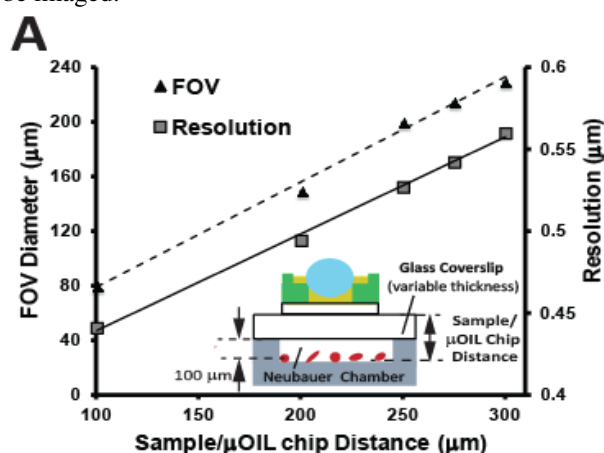


Figure 3. (A) FOV and resolution versus sample/ $\mu\text{OIL}$  chip distance. The FOV is the diameter of the area that a single sapphire lens can visualize. (B) An image of RBCs as captured through our system for a sample/ $\mu\text{OIL}$  chip distance of 200  $\mu\text{m}$ . Scale bar, 50  $\mu\text{m}$ .

The FOV in our system can be modified by changing the distance between the bottom surface of the  $\mu$ OIL chip and the sample. To estimate that dependence, we used the grid pattern of the Neubauer chamber as a reference sample, placed it at 100, 150, 175 and 200  $\mu\text{m}$  below the bottom surface of the  $\mu$ OIL chip and measured the corresponding FOV. We used glass coverslips of different thicknesses to vary the sample/ $\mu$ OIL chip distance. We also performed optical simulations in OSLO software to estimate the corresponding resolution (Fig. 3).

As expected, the larger the sample/ $\mu$ OIL chip distance the larger the FOV and lower the resolution. For our RBC counting experiments as explained earlier, we selected a FOV of  $\sim 200 \mu\text{m}$  as it matches the standardized,  $200 \mu\text{m} \times 200 \mu\text{m}$  imaging area of the Neubauer chamber (depicted in Fig. 2B). The resolution and NA in this case were estimated to be  $0.53 \mu\text{m}$  and  $0.54$  respectively.

### Comparing RBC counts

We obtained images from diluted whole blood samples with our system and with a microscope (Fig. 4) as described earlier. In both cases, we used a haemocytometer with a  $150 \mu\text{m}$  thick glass coverslip.

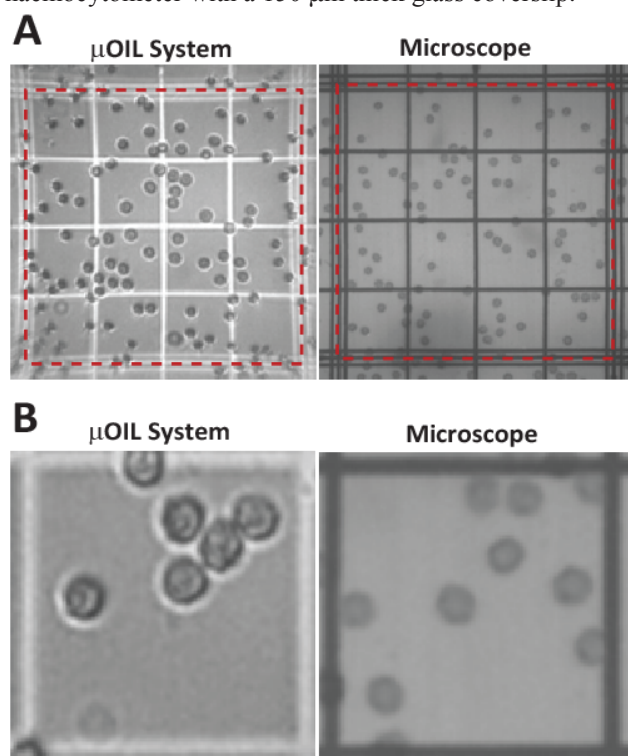


Figure 4. (A) Diluted blood samples as imaged through our system ( $NA=0.54$ ) (left) and a microscope with  $50\times$  ( $NA=0.5$ ) objective (right). (B) Magnified images from a single  $50 \mu\text{m} \times 50 \mu\text{m}$  square of the grid containing RBCs. The dimple of the RBCs is visible with the  $\mu$ OIL system.

We noticed that, although the NA of the  $\mu$ OIL system and the microscope are similar ( $0.54$  versus  $0.5$ ), the  $\mu$ OIL system could resolve details of the cell geometry/size much better than the microscope (Fig. 4B). The biconcave RBC shape with the characteristic dimple in the middle was clearly visible. We believe that the

main reason for such a difference on the image quality is due to the high contrast that is generated by the bright-field illumination of our system. We also noticed that the sapphire lens of  $\mu$ OIL system distorts the edges of the viewing area. That effect did not alter the RBC counting results as cells are still identifiable.

We furthermore performed imaging experiments with blood samples diluted by three different factors (50, 100 and 200) (Fig. 5). For all 3 dilution factors, we did not observe any significant differences between the RBC counts obtained with the microscope and our system.

We also compared our system with a flow cytometer which is considered the gold standard for cell counting applications. The flow cytometer count was  $4.57$  million cells/ $\mu\text{L}$  (see dotted line in Fig. 5, no dilution). The RBC count from our system is in good agreement with the flow cytometer results within one standard deviation for dilution factors of 50 and 100. RBC counts with larger (e.g.  $>200$ ) dilution factors are not recommended as there is a significant difference ( $\sim 10\%$  error) between the flow cytometry and  $\mu$ OIL system results. However, standard haemocytometer-based RBC counting procedures recommend a dilution factor of 200 to facilitate the manual counting process. We should also note that despite the fact that we used whole blood, the presence of white blood cells (WBCs) does not affect the RBC count as WBCs make up only  $0.1\%$  of the total number of cells in blood and as a result they rarely appear in the images.

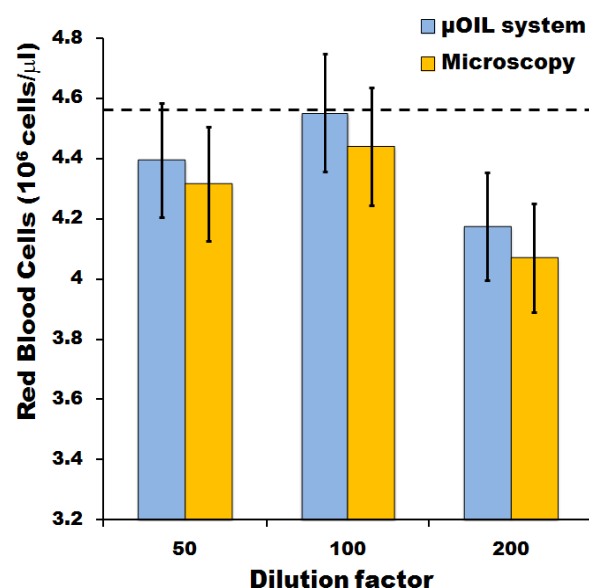


Figure 5. Comparing RBC counts. The dotted line is the RBC count ( $4.57 \times 10^6$  cell/ $\text{mL}$ ) as measured by flow cytometry. The error bars represent one standard deviation.

### CONCLUSION

We developed a high resolution, compact, single-cell imaging system for counting cells. The imaging capabilities of the system can be attributed to the use of a high NA microfabricated lens array. Although we demonstrated counting results from a single lens, we anticipate that the use of the entire lens array will automate the counting process and eliminate statistical variations as the sample size (number of cells counted)



will significantly increase. We believe that the use of our system is not limited to cell imaging/counting but it can be expanded to imaging other biological samples such as bacteria, microbes, microorganisms and tissue samples as it provides excellent image quality that is comparable to the one obtained from high end microscopes.

## ACKNOWLEDGEMENTS

This research was made possible with the support of the NIH Microfluidics in Biomedical Sciences Training Program, the Macromolecular Science and Engineering program and the 2009 NIH Director's New Innovator Award. We would also like to thank Lindsay Szczepanski at the UofM Hematology lab, the UofM medical school for providing and analyzing blood samples via flow cytometer and Marv Cressey for helping with the prototype. All the devices were fabricated at the UofM Lurie Nanofabrication Facility.

## REFERENCES:

- [1] "WHO | Micronutrient deficiencies." [Online]. Available: <http://www.who.int/nutrition/topics/ida/en/>. [Access:25-Mar-2013].
- [2] "Complete Blood Count: The Test." [Online]. Available: <http://labtestsonline.org/understanding/analytes/cbc/tab/test>. [Accessed: 25-Mar-2013].
- [3] B. Kuswandi, Nuriman, J. Huskens, and W. Verboom, "Optical sensing systems for microfluidic devices: a review.," *Analytica chimica acta*, vol. 601, no. 2, pp. 141–55, Oct. 2007.
- [4] H. Zhu, S. O. Isikman, O. Mudanyali, A. Greenbaum, and A. Ozcan, "Optical imaging techniques for point-of-care diagnostics.," *Lab on a chip*, vol. 13, no. 1, pp. 51-67, 2013.
- [5] K. Roberts, "A silicon microfabricated aperture for coating cells using the aperture impedance technique", *M.S. thesis Dept. Applied Science., Simon Fraser Univ., Canada*. June, 1999.
- [6] H. Zhu, O. Yaglidere, T.-W. Su, D. Tseng, and A. Ozcan, "Cost-effective and compact wide-field fluorescent imaging on a cell-phone", *Lab on a chip*, vol. 11, no. 2, pp. 315–22, Jan. 2011.
- [7] X. Heng, D. Erickson, L. R. Baugh, Z. Yaqoob, P. W. Sternberg, D. Psaltis, and C. Yang, "Optofluidic microscopy--a method for implementing a high resolution optical microscope on a chip", *Lab on a chip*, vol. 6, no. 10, pp. 1274–6, Oct. 2006.
- [8] S. Moon, H. O. Keles, A. Ozcan, A. Khademhosseini, E. Haeggstrom, D. Kuritzkes, and U. Demirci, "Integrating microfluidics and lensless imaging for point-of-care testing", *Biosensors & bioelectronics*, vol. 24, no. 11, pp. 3208–14, Jul. 2009.
- [9] U. A. Gurkan, S. Moon, H. Geckil, F. Xu, S. Wang, T. J. Lu, and U. Demirci, "Miniaturized lensless imaging systems for cell and microorganism visualization in point-of-care testing", *Biotechnology journal*, vol. 6, no. 2, pp. 138–49, Feb. 2011.

- [10] M. N. Gulari, A. Tripathi, and N. Chronis, "Microfluidic-based oil-immersion lenses for high resolution microscopy", *The 16<sup>th</sup> International Conference on Miniaturized Systems for Chemistry and Life Sciences ( $\mu$ TAS'12)*, Okinawa, Japan, October 28 - November 1, 2012, pp. 49–51.
- [11] E. Pascual and V. Jovaní, "Synovial fluid analysis.," *Best practice & research. Clinical rheumatology*, vol. 19, no. 3, pp. 371–86, Jun. 2005.
- [12] M. C. Phelan<sup>1</sup> and G. Lawler, "Cell Counting - Current Protocols", *Current Protocols in Cytometry*, 2001.

## CONTACT

\*N. Chronis, tel: +1-734- 763-0154; [chronis@umich.edu](mailto:chronis@umich.edu)